REPORT DOCUMENTATION PAGE

Form Approved OMB NO. 0704-0188

1. REPORT DATE (DD-MM-YYYY)	2. REPORT TYPE	3. DATES COVERED (From - To)
28-02-2011	Final Report	25-Aug-2006 - 31-May-2010

4. TITLE AND SUBTITLE
Multifunctional Metallosupramolecular Materials

5a. CONTRACT NUMBER
W911NF-06-1-0414

5b. GRANT NUMBER

5c. PROGRAM ELEMENT NUMBER
611102

6. AUTHORS
Stuart Rowan, Christoph Weder

5d. PROJECT NUMBER

5e. TASK NUMBER

5f. WORK UNIT NUMBER

7. PERFORMING ORGANIZATION NAMES AND ADDRESSES
Case Western Reserve University
10900 Euclid Avenue
415 Glennan Building
Cleveland, OH 44106 -

8. PERFORMING ORGANIZATION REPORT NUMBER

9. SPONSORING/MONITORING AGENCY NAME(S) AND ADDRESS(ES)
U.S. Army Research Office
P.O. Box 12211
Research Triangle Park, NC 27709-2211

10. SPONSOR/MONITOR'S ACRONYM(S)
ARO

11. SPONSOR/MONITOR'S REPORT NUMBER(S)
50464-CH.8

12. DISTRIBUTION AVAILIBILITY STATEMENT
Approved for Public Release; Distribution Unlimited

13. SUPPLEMENTARY NOTES
The views, opinions and/or findings contained in this report are those of the author(s) and should not contrued as an official Department of the Army position, policy or decision, unless so designated by other documentation.

14. ABSTRACT
The development of new polymer materials, which exhibit significantly enhanced mechanical and thermal properties, offer new functions such as adaptability and self-healing capability, and are easy to manufacture and process will enable numerous applications that are vital to the Army and other DoD branches. This research reported herein outlines the development of new metallo-supramolecular polymers that are the basis of (1) high temperature stable materials, and (2) photo and thermal responsive re-healable systems (3) mechanical stable light

15. SUBJECT TERMS
Metallosupramoelcular Polymers, Photohealing, poly(p-xylylene), poly(p-phenylene ethynylene)

16. SECURITY CLASSIFICATION OF:			17. LIMITATION OF ABSTRACT	15. NUMBER OF PAGES	19a. NAME OF RESPONSIBLE PERSON
a. REPORT	b. ABSTRACT	c. THIS PAGE			Stuart Rowan
UU	UU	UU	UU		19b. TELEPHONE NUMBER: 216-368-4242

Report Title

Multifunctional Metallosupramolecular Materials

ABSTRACT

The development of new polymer materials, which exhibit significantly enhanced mechanical and thermal properties, offer new functions such as adaptability and self-healing capability, and are easy to manufacture and process will enable numerous applications that are vital to the Army and other DoD branches. This research reported herein outlines the development of new metallo-supramolecular polymers that are the basis of (1) high temperature stable materials, and (2) photo and thermal responsive re-healable systems (3) mechanical stable light emitting materials. These interrelated thrusts exploit the noncovalent interactions between metals and macromonomers based on the bis-(benzimidazolyl)pyridine (Bip) ligand. The properties of the resulting self-assembled polymers depend on the nature of the non-covalent self-assembly process and the nature of the macromonomer and can be readily tailored.

List of papers submitted or published that acknowledge ARO support during this reporting period. List the papers, including journal references, in the following categories:

(a) Papers published in peer-reviewed journals (N/A for none)

Burnworth M., Rowan S.J., Weder C. Fluorescent Sensors for the Detection of Chemical Warfare Agents Chem. Eur. J. 2007, 13, 7828-7836.

Burnworth, M.; Mendez, J.D., Schroeter, M.; Rowan, S.J.; Weder, C. Decoupling Optical Properties in Metallo-Supramolecular Poly(p-phenylene ethynylene)s Macromolecules 2008, 41, 2157-2163.

Wojtecki, R.J.; Meador, M.A.; Rowan S.J. Utilizing the Dynamic Bond to Access Macroscopically-Responsive Structurally-Dynamic Polymers Nature Materials 2011, 10, 14-27.

Burnworth, M.; Tang, L.; Kumpfer, J.R., Duncan, A. J., Beyer, F.L.; Rowan S.J.; Weder, C. Optically Healable Supramolecular Polymers Nature 2011, accepted.

Number of Papers published in peer-reviewed journals: 4.00

(b) Papers published in non-peer-reviewed journals or in conference proceedings (N/A for none)

Number of Papers published in non peer-reviewed journals: 0.00

(c) Presentations

Rowan
Nov 2010 University of Cambridge, Cambridge UK
Invited Lecture: Supramolecular Approaches to Stimuli-Responsive Materials: From Sea Cucumbers to Self-Healing Films.
Oct 2010 University of Wisconsin, Madison, USA
Invited Lecture: Using Supramolecular Chemistry to Access Stimuli-responsive Materials
Oct 2010 Johns Hopkins University, Baltimore, USA
Invited Lecture: Using Supramolecular Chemistry to Access Stimuli-responsive Materials
Sept 2010 Louisiana State University, Baton Rouge, USA
Invited Lecture: Supramolecular Approaches to Stimuli-responsive Materials
Aug 2010 ACS Fall Meeting, Boston
Invited Lecture: Utilizing Supramolecular Interactions to Access Dynamic Materials
June 2010 Gordon Research Conference: Polymer Physics, Mt Holyoke, Massachusetts
Invited Lecture: Utilizing Supramolecular Interactions to Access Dynamic Materials
May 2010 Center for the Chemistry of Integrated Systems, Northwestern University, Illinois
Invited Lecture: Utilizing Supramolecular Interactions to Access Dynamic Materials
May 2010 Kent State University, Kent, Ohio
Invited Lecture: Utilizing Supramolecular Interactions to Access Dynamic Materials
Mar 2010 University of Colorado, Colorado
Invited Lecture: Utilizing Supramolecular Interactions to Access Dynamic Materials
Mar 2010 IBM Almaden Research Center, San Jose, CA
Invited Lecture: Utilizing Supramolecular Interactions to Access Dynamic Materials
Mar 2010 ACS Spring Meeting, San Francisco
Invited Lecture: Utilizing Supramolecular Interactions to Access Dynamic Materials
Feb 2010 University of South Carolina, Department of Chemistry, Columbia, SC
Invited Lecture: Using Supramolecular Interactions to Access Dynamic Materials
Feb 2010 Tulane University, Department of Chemistry, New Orleans, LA
Invited Lecture: Using Supramolecular Interactions to Access Dynamic Materials
Jan 2010 University of Rochester, Department of Chemical Engineering, Rochester, NY
Invited Lecture: Using Supramolecular Interactions to Access Dynamic Materials
Dec 2009 RSC Supramolecular and Macrocycles Meeting, Cambridge, UK
Plenary Lecture: Using Supramolecular Interactions to Access Dynamic Materials
Oct 2009 Southern Methodist University, Dallas, Texas
Invited Lecture: Supramolecular Chemistry in Polymeric Systems: From Nanoassemblies to Dynamic Materials
Aug 2009 ACS Fall Meeting, Washington DC
Invited Lecture: Stimuli-responsive metallo-supramolecular polymers
July 2009 Gordon Conference on Supramolecules and Assemblies
Invited Lecture: Using Supramolecular Interactions to Access Dynamic Materials
May 2009 University of Cincinnati, Cincinnati, Ohio
Invited Lecture: Supramolecular Chemistry in Polymeric Systems: From Nanoassemblies to Dynamic Materials
April 2009 University of Michigan, Ann Arbour, Michigan
Invited Lecture: Supramolecular Chemistry in Polymeric Systems: A Route to Responsive Materials
March 2009 ACS Spring Meeting, Salt Lake, Utah
Invited Lecture: Toward applications for metallosupramolecular polymers
Feb 2009 Smart Coatings, Orlando, Florida
Invited Lecture: Supramolecular Chemistry in Polymeric Systems: Route to Responsive Materials
Feb 2009 Texas Tech., Lubbock, Texas
Invited Lecture: Supramolecular Chemistry in Polymeric Systems: Route to Responsive Materials
Feb 2009 New York University, New York
Invited Lecture: Supramolecular Materials: From Gels to Self-healing Polymers
Dec 2008 Lubrizol, Wickliffe, Ohio
Invited Lecture: Supramolecular Materials: From Re-healable Plastics to Sea Cucumbers
Dec 2008 US-Japan Polymer Chemistry Symposium, Awaji Island, Japan
Invited Lecture: Investigating How Supramolecular Interactions Can Influence and Control Polymer Properties
Oct 2008 Montana State University, Department of Chemistry
Invited Lecture: Utilizing Supramolecular Chemistry in Polymeric Systems: A Route to Dynamic, Adaptive Materials
Oct 2008 New York University, Department of Chemistry

Invited Lecture: Supramolecular Chemistry in Polymeric Systems: From Nanoassemblies to Dynamic Materials
Sept 2008 College of Wooster, Department of Chemistry
Invited Lecture: Supramolecular Polymer Chemistry: A Route to Responsive Materials
Aug 2008 Goodyear, Akron, Ohio
Invited Lecture: Supramolecular Polymers for Flexible Healable Materials
June 2008 CERMACS, Columbus, Ohio,
Invited Lecture: Supramolecular Chemistry in Polymeric Systems
June 2008 Molecular Nanotechnology 2008, University of Reading, UK
Invited Lecture: Accessing and Utilizing Molecular Nano-scaffolds
May 2008 University of Minnesota IPRIME Workshop, University of Minnesota, USA
Invited Lecture: Using Non-covalent Interactions to Access Dynamic Materials.
April 2008 American Chemical Society Meeting, New Orleans, USA
Invited Lecture: Metallo-supramolecular polymers and gels: A dynamic class of organic/inorganic hybrid polymers.
March 2008 Goodyear, Akron, Ohio
Invited Lecture Supramolecular Polymers: From Dynamic Chemistry to Dynamic Materials
Feb 2008 Department of Chemistry, The Ohio State University, USA
Invited Lecture: Supramolecular Polymers: From Dynamic Chemistry to Dynamic Materials.
Oct 2007 Department of Material Science and Engineering, University of Delaware, USA
Invited Lecture: Utilizing Specific Supramolecular Interactions to Access New Responsive Materials.
Aug 2007 American Chemical Society Meeting, Boston, USA
Invited Lecture: Investigations into supramolecular polymer architectures.
Aug 2007 American Chemical Society Meeting, Boston, USA
Invited Lecture: Investigating the Effects of Lanthanide ions in Metallosupramolecular Polymers and Gels
Aug 2007 American Chemical Society Meeting, Boston, USA
Invited Lecture: Investigations into New Supramolecular Polymers

Weder
Invited Lecture: “How to teach polymers new tricks”
Micronarc Industrial Forum, November 10, 2010, Fribourg, Switzerland
Invited Lecture: “Les matériaux intelligents du futur”
Friburgissima, September 27, 2010, Fribourg, Switzerland
Invited Seminar: “Current Trends in Polymer-Based Nanomaterials”
Firmenich; June 14, 2010; Geneva, Switzerland
Invited Seminar: Current Trends in Polymer-Based (Nano) materials
Apr. 2010 BASF; Ludwigshafen, Germany
Keynote Lecture: Functional Polymer Blends and Nanocomposites
Nov 2009 Assemblée Generale Reseau Plasturgie, Fribourg Switzerland
Keynote Lecture: Mechanically Adaptive Polymer Nanocomposites
Sept 2009 Trends in Nanotechnology TNT 2009, Barcelona, Spain
Invited Seminar: Supramolecular Metallopolymers
May 2009 Chulalongkorn University, Bangkok, Thailand
Invited Seminar: Noncovalent Interactions as a Design Tool for Functional Polymers
Jan 2009 University of Southern Mississippi, Department of Polymer Science and Engineering, January 29, 2009; Hattiesburg, MS
Invited Seminar: “Noncovalent Interactions as a Design Tool for Functional Polymers”
University of Tokyo, Dept. of Chemistry; December 14, 2007; Tokyo, Japan
Invited Lecture: “Metallosupramolecular Conjugated Polymers”
The Third International Symposium on Chemistry of Coordination Space ISCCS 2007; December 9 – 12, 2007; Awaji, Hyogo, Japan
Invited Seminar: “Noncovalent Interactions as a Design Tool for Functional Polymers”
Princeton University, Dept. of Chemistry; November 29, 2007; Princeton, NJ

Burnworth
June 2009 2nd International Conference on Self-Healing Materials 2009Opitically Responsive Metallopolymers

Number of Presentations: 52.00

Non Peer-Reviewed Conference Proceeding publications (other than abstracts):

Number of Non Peer-Reviewed Conference Proceeding publications (other than abstracts): 0

Peer-Reviewed Conference Proceeding publications (other than abstracts):

Number of Peer-Reviewed Conference Proceeding publications (other than abstracts): 0

(d) Manuscripts

Number of Manuscripts: 0.00

Patents Submitted

Patents Awarded

Awards

Stuart Rowan: Fellow of the Royal Society of Chemistry (FRSC)

Graduate Students

NAME	PERCENT_SUPPORTED
Mark Burnworth	1.00
FTE Equivalent:	**1.00**
Total Number:	**1**

Names of Post Doctorates

NAME	PERCENT_SUPPORTED
FTE Equivalent:	
Total Number:	

Names of Faculty Supported

NAME	PERCENT_SUPPORTED	National Academy Member
Stuart Rowan	0.02	No
Christoph Weder	0.02	No
FTE Equivalent:	**0.04**	
Total Number:	**2**	

Names of Under Graduate students supported

NAME	PERCENT_SUPPORTED
FTE Equivalent:	
Total Number:	

Student Metrics

This section only applies to graduating undergraduates supported by this agreement in this reporting period

The number of undergraduates funded by this agreement who graduated during this period:	0.00
The number of undergraduates funded by this agreement who graduated during this period with a degree in science, mathematics, engineering, or technology fields:.....	0.00
The number of undergraduates funded by your agreement who graduated during this period and will continue to pursue a graduate or Ph.D. degree in science, mathematics, engineering, or technology fields:.....	0.00
Number of graduating undergraduates who achieved a 3.5 GPA to 4.0 (4.0 max scale):	0.00
Number of graduating undergraduates funded by a DoD funded Center of Excellence grant for Education, Research and Engineering:	0.00
The number of undergraduates funded by your agreement who graduated during this period and intend to work for the Department of Defense	0.00
The number of undergraduates funded by your agreement who graduated during this period and will receive scholarships or fellowships for further studies in science, mathematics, engineering or technology fields:	0.00

Names of Personnel receiving masters degrees

NAME
Total Number:

Names of personnel receiving PHDs

NAME
Mark Burnworth
Total Number: 1

Names of other research staff

NAME	PERCENT_SUPPORTED
FTE Equivalent:	
Total Number:	

Sub Contractors (DD882)

Inventions (DD882)

Scientific Progress

See Attachment

Technology Transfer

Scientific progress and accomplishments

Multifunctional Metallosupramolecular Materials

1. Introduction

The ability to exploit non-covalent interactions for the self-assembly of polymeric aggregates, i.e. supramolecular polymerization, opens the door to novel materials that exhibit a range of unusual mechanical properties. The goal of this project is to investigate the potential of one distinct class of supramolecular polymers to impact two distinct areas relevant to DoD applications, namely easy-to-process materials with good high-temperature stability and a novel class of photo-healable plastics. More specifically, we are interested in metallo-supramolecular polymers that consist of telechelic macromonomers with 2,6-bis(1'-methyl-benzimidazolyl)pyridine (Mebip) ligands attached to their termini. These building blocks can be self-assembled with a variety of different metal ion salts (**Figure 1**). The core of the macromonomer and the nature of metal ion salt utilized can be varied to tailor the material's properties to meet the specific needs of the respective application. For the processable high temperature materials the high thermally stable poly(*p*-xylylene) (PPX) is used as the macromonomer core, while for the photo-healable plastics a low-T_g hydrogenated poly(butadiene) (i.e. poly(ethylene butylene) was selected as the core unit.

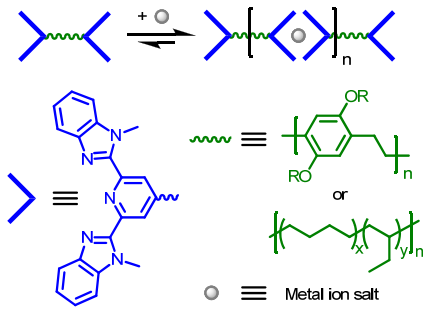

Figure 1. Schematic representation of the metallo-supramolecular polymers investigated in this study.

2. Results and Discussion

2.1. Easy-To-Process Materials with Good High-Temperature Stability (Paper to be submitted)

There has been an increasing interest in the use of metal-ligand binding as the thermodynamic driving force for the self-assembly of ditopic ligands into supramolecular polymers.[1] Previous work by Knapton et al demonstrated that the combination of metal-ligand interactions with thermally stable building blocks can yield materials which are easy to process and offer outstanding mechanical properties over a wide temperature regime.[2] The previously studied materials system was composed of two different building blocks that could self-assemble into a variety of polymeric architectures and include a highly stable polymer backbone, and a ligand unit that allows coordination to a variety of metal centers.

The polymer building blocks utilized in previous studies are based on poly(arylene alkylene) moieties, which offer a unique combination of outstanding thermal and mechanical properties and high chemical stability.[3] Poly(*p*-xylylene) (PPX)[4] is the most prominent representative of the poly(arylene alkylene) family. This polymer and its derivatives are well-known for an appealing combination of high thermal stability, excellent solvent resistance, high degree of crystallinity, low dielectric permittivity, and outstanding barrier properties.[5,6] In addition, PPX exhibits excellent mechanical properties with a Young's modulus and a tensile strength of ca. 2.4 GPa and 47 MPa, respectively.[5] Thus, PPX is an attractive material for many applications, including packaging of electronic components, medical device fabrication, and artifact conservation.[5] Unfortunately, broad industrial exploitation of PPX has been stifled on account of its intractability. Its high melting temperature (424 °C, which overlaps with the onset of thermal degradation) and poor solubility make conventional processing protocols virtually impossible.[7,8] As a result, the only practical approach for the synthesis and processing of PPX is by chemical vapor deposition polymerization.[9]

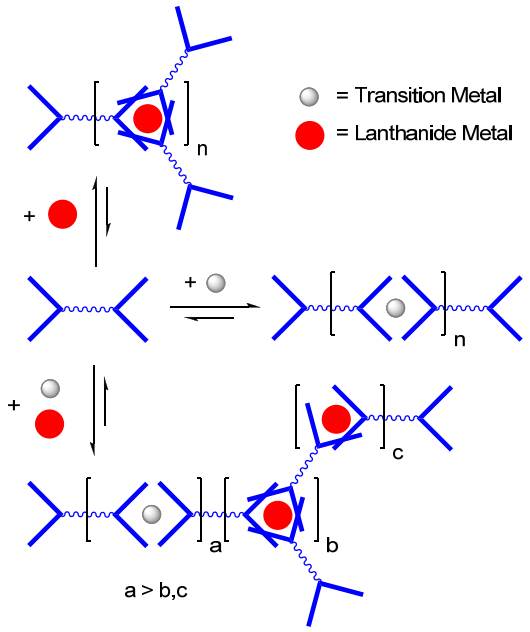

Figure 2. Schematic representation of the metallo-supramolecular polymerization of ditopic ligands with either transition or lanthanide metal ions.

This part of the project describes efforts to exploit the 2,6-bis(1'-methyl-benzimidazolyl)pyridine (Mebip) ligand as the metal binding unit, in conjunction with metal ions to template the formation of metallo-supramolecular metallosupramolecular PPX. The Mebip ligand is easy to prepare and permits access to wide range of structural derivatives,[10] allowing it to be incorporated into the desired range of polymeric structures. In addition, Mebip binds to a wide range of transition and lanthanoid metal ions, offering extensive tuneability in kinetic and thermodynamic stability of the resulting polymeric architectures (Figure 2).

Previous work in this area by Knapton et al. reported that the metallo-supramolecular polymerization of thermally stable Mebip end-capped poly(arylene alkylene) macromonomers did not produce self-supporting films with addition of either $Zn(ClO_4)_2$ or $Fe(ClO_4)_2$. However, with a combination of $La(ClO_4)_3$, which acts as a crosslinker, and $Fe(ClO_4)_2$ mechanically stable films were produced. The mechanically stable films were easy to process and displayed high thermal stability, with good mechanical properties. Expanding on this previous work, further experiments were conducted to explore the both the effects of the counterion and the nature of the crosslinker in order to increase thermal stability. This Chapter summarizes our recent results regarding (1) the optimization of the synthesis and purification protocols for the Mebip-terminated PPX macromonomer, (2) the properties of materials prepared from the latter, (3) the influence of the nature of the metal ion salt, and (4) the influence of a tetravalent Mebip end-capped crosslinking agent.

Synthesis and Characterization of Macromonomer 1. The synthetic protocol utilized to access the 2,6-bis(1'-methylbenzimidazoyl) pyridine end-capped 2,5-dialkoxy-*p*-xylylene macromonomer (**1**) involves the Hahn diimide reduction of the parent conjugated 2,5-dialkoxy-*p*-phenyleneethynylene **2**, which was prepared in greater than 90% yield via the Sonogashira coupling reaction of acetylenes **3**, **5** and aryl diiodide **4**. As previously reported by Knapton et al.,[2] the purification of **1** was achieved via precipitation into MeOH and washing with boiling MeOH, EtOH, CH_3CN and room-temperature MeOH (Figure 3, method A) to yield the desired compound **1** in 70% yield. Although this method produced **1** in good yield, *p*-toluenesulfinic acid remained in the product as evidenced by ^{1}H NMR. The impurity peak at 2.32 ppm, originally designated as toluene, is characteristic of the methyl group of *p*-toluenesulfinic acid and re-examination of the previously published[2] spectra showed it was present in a concentration of 133 mol% (2.1% w/w) relative to the macromonomer (Figure 4a). To overcome this problem, the purification procedure was optimized to completely remove this reaction byproduct. The new purification method involves precipitation in EtOH (2x) and washing with boiling MeOH, EtOH, CH_3CN, and diethyl ether to isolate the desired compound **1** in 63 % yield and free of the characteristic *p*-toluenesulfinic acid peak at 2.32 ppm (Figure 3, method B, Figure 4.1b).

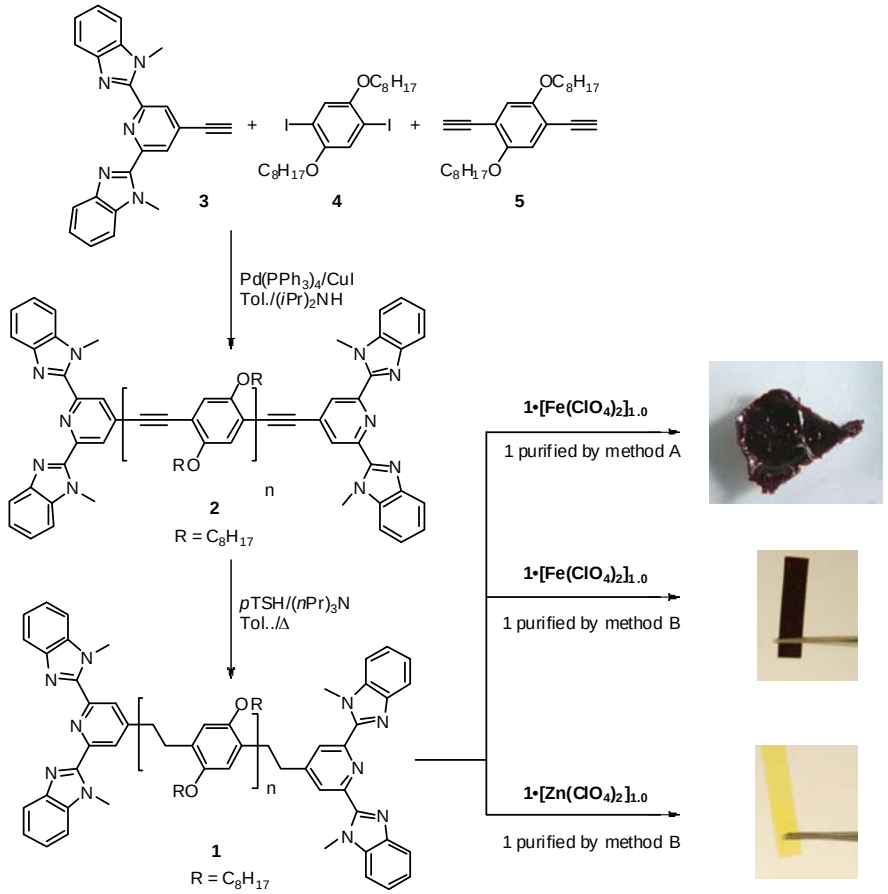

Figure 3. Synthesis and structure of the conjugated monomer **2**, its reduction to the ditopic macromonomer **1**, and pictures of the films obtained upon solution casting supramolecular metallopolymers of **1** with equimolar amounts of either $Fe(ClO_4)_2$ or $Zn(ClO_4)_2$. The properties of the resulting films depend on the procedure used to purify **1**.

We determined that monitoring a titration experiment, involving the addition of metal ions into the macromonomer, with UV-Vis spectroscopy is the most accurate pathway to molecular weight calculation (or at least allows a more accurate determination at what metal ion content all the ligands are complexed). In this experiment a solution of **1** (50 μM) was slowly titrated with a solution of $Fe(ClO_4)_2$ while maintaining a constant concentration of **1** (Figure 5). As the metal ion was added to the macromonomer the absorption spectrum changes from that of the free Mebip ligand to that of the Mebip:Fe^{2+} complex. When all Mebip ligands are complexed with Fe^{2+} the changes of the absorbance spectrum level off. The metal ion concentration that corresponds to the leveling off of the absorption spectrum can then be used to back-calculate the molecular weight of **1**. This method has been determined to obtain a more accurate molecular weight than ^{1}H end-group analysis.

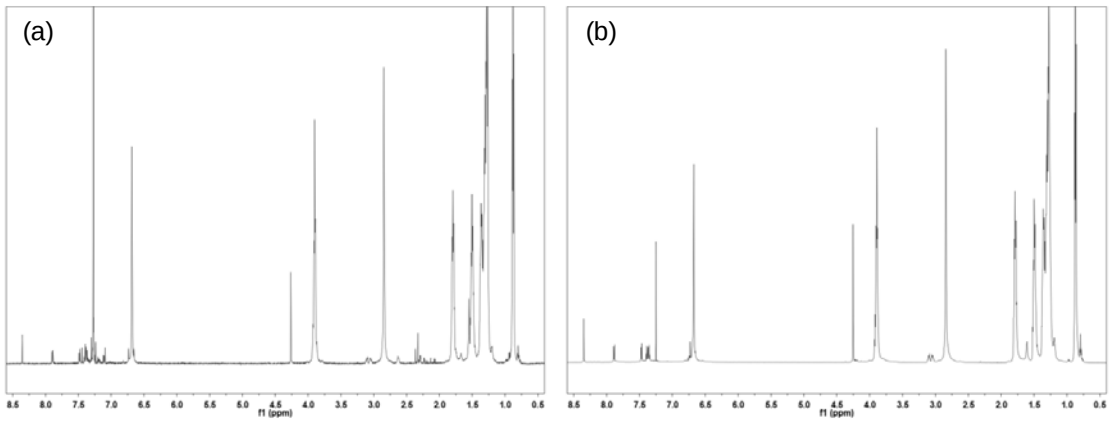

Figure 4. ^{1}H NMR of macromonomer **1**, conducted at 25 °C in $CDCl_3$, (a) as synthesized by method A, and (b. method B.

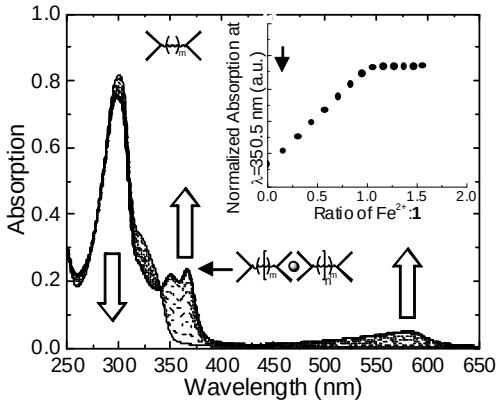

Figure 5. UV-Vis absorption spectra acquired upon titration of **1** (50 μM) with $Fe(ClO_4)_2$. Shown are spectra at selected Fe^{2+}:**1** ratios ranging from 0:1 to 1.5:1. The insets show the normalized absorption at 350.5 nm as a function of Fe^{2+}:**1** ratio.

To investigate the influence of the purification procedure and the molecular weight calculation (the latter leading to a better stoichiometric ratio of metal and macromonomer) on the mechanical properties of the metallo-supramolecular polymers made from **1**, thin films were prepared by solution casting **1** with one molar equivalent of either $Fe(ClO_4)_2$, $Zn(ClO_4)_2$, $Zn(OTf)_2$, or $Zn(NTf_2)_2$ (**1·[Fe(ClO$_4$)$_2$]$_{1.0}$**, **1·[Zn(ClO$_4$)$_2$]$_{1.0}$**, **1·[Zn(OTf)$_2$]$_{1.0}$**, **1·[Zn(NTf$_2$)$_2$]$_{1.0}$**), in addition a film (**1·[La(NTf$_2$)$_3$]$_{1.0}$**) was prepared with 0.66 molar equivalents of $La(NTf_2)_3$, assuming 3 ligands bound per metal ion. Employment of the new purification and molecular weight calculation techniques allowed the fabrication of metallo-supramolecular polymer films from different metals and counterions with appreciable mechanical (Figure 3). This represents a significant progress compared to the materials produced with the originally reported method,[2] which in the case of $Fe(ClO_4)_2$, resulted only a brittle material. It appears that *p*-toluenesulfinic acid, albeit in a small weight percentage (2.1% w/w), acted as a competitive binder with the Mebip ligand, in our original material, which in combination with a less accurate molecular weight calculation led to an offset of the metal/ligand ratio, concomitant with a significant effect on the mechanical properties.

Thermogravimetric Analysis. The thermal stability of **1**, and resulting metallo-supramolecular polymers **1·[Fe(ClO$_4$)$_2$]$_{1.0}$**, **1·[Zn(ClO$_4$)$_2$]$_{1.0}$**, **1·[Zn(OTf)$_2$]$_{1.0}$**, **1·[Zn(NTf$_2$)$_2$]$_{1.0}$**, and **1·[La(NTf$_2$)$_3$]$_{0.66}$** were investigated by thermogravimetric analysis (TGA) (Figure 6). It was found that the neat macromonomer, **1**, was thermally stable up ca. 350 °C, and subsequently degraded with 90% weight loss by 500 °C. Metallo-supramolecular polymers **1·[Zn(OTf)$_2$]$_{1.0}$**, **1·[Zn(NTf$_2$)$_2$]$_{1.0}$**, and **1·[La(NTf$_2$)$_3$]$_{0.66}$**, all showed similar trends with an onset of weight loss occurring ca. 350 °C, and a single weight loss peak occurring from 350-500 °C. The two metallo-supramolecular polymers with the less thermally stable perchlorate counterion showed degradation at lower temperatures. The **1·[Fe(ClO$_4$)$_2$]$_{1.0}$** film exhibited 2.5 wt.% loss at ca. 190 °C, while the **1·[Zn(ClO$_4$)$_2$]$_{1.0}$** film displayed 2.7 wt.% loss at 285 °C, both transitions are attributed to the degradation of the perchlorate counterion. Both **1·[Fe(ClO$_4$)$_2$]$_{1.0}$** and **1·[Zn(ClO$_4$)$_2$]$_{1.0}$** displayed major weight loss at ca. 350-500 °C, similar to the other metallo-supramolecular polymers.

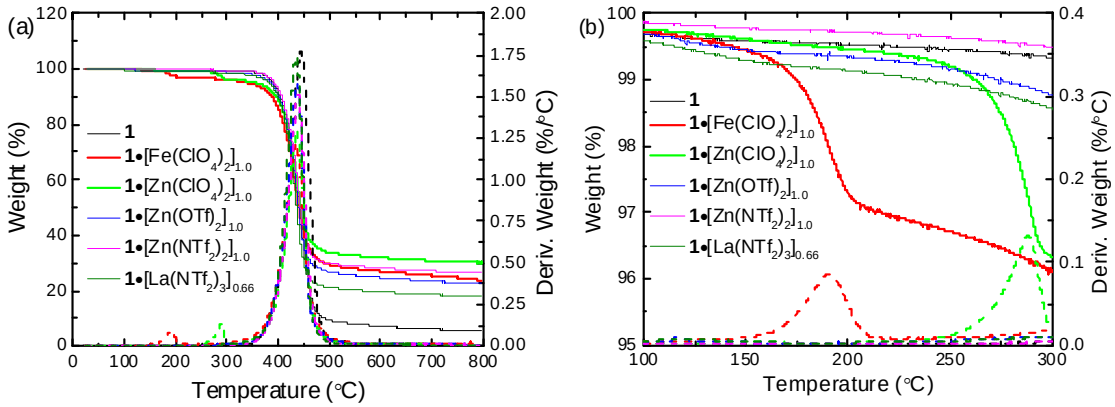

Figure 6. (a,b) Thermogravimetric analysis (TGA) trace for neat macromonmer **1** (black), **1·[Fe(ClO$_4$)$_2$]$_{1.0}$** (red), **1·[Zn(ClO$_4$)$_2$]$_{1.0}$** (green), **1·[Zn(OTf)$_2$]$_{1.0}$** (blue), **1·[Zn(NTf$_2$)$_2$]$_{1.0}$** (magenta), and **1·[La(NTf$_2$)$_3$]$_{0.66}$** (olive). The experiments were conducted at a heating rate of 10 °C/min under N_2.

Differential Scanning Calorimetry. Thermal transitions for the neat macromonomer **1**, and the resulting metallo-supramolecular polymers **1·[Zn(ClO$_4$)$_2$]$_{1.0}$**, **1·[Zn(OTf)$_2$]$_{1.0}$**, **1·[Zn(NTf$_2$)$_2$]$_{1.0}$**, and **1·[La(NTf$_2$)$_3$]$_{0.66}$** were investigated by differential scanning calorimetry (DSC). The neat macromonomer **1** (Figure 7a) displayed a glass transition temperature (T_g) of ca. 50 °C, and a reversible endotherm with a maximum at 164 °C. All metallo-supramolecular films tested displayed similar thermal transitions with T_g occurring at ca 50 °C and a reversible endotherm at 164 ± 4 °C (Figure 3.4b, Figure A3.5). The reversible endotherm displayed by both neat **1**, and the resulting metallo-supramolecular polymers is related to polymeric backbone, and it ascribed to either the melting temperature (T_m) of the polymeric backbone or the T_m alkyl side chains, which have shown to possess polyethylene-type ordering in the parent poly(phenylene ethynylene)s.[11] In these materials the counterion did not significantly affect the temperature at which these transitions occur nor did changing from the Zn^{2+} system to La^{3+} system, which along with the DSC data of the macromonomer **1** suggests that these thermal transitions in the metallosupramolecular polymer originate from its macromonomer core. The **1·[Fe(ClO$_4$)$_2$]$_{1.0}$** film was not tested on account of the lower degradation temperature associated with this film.

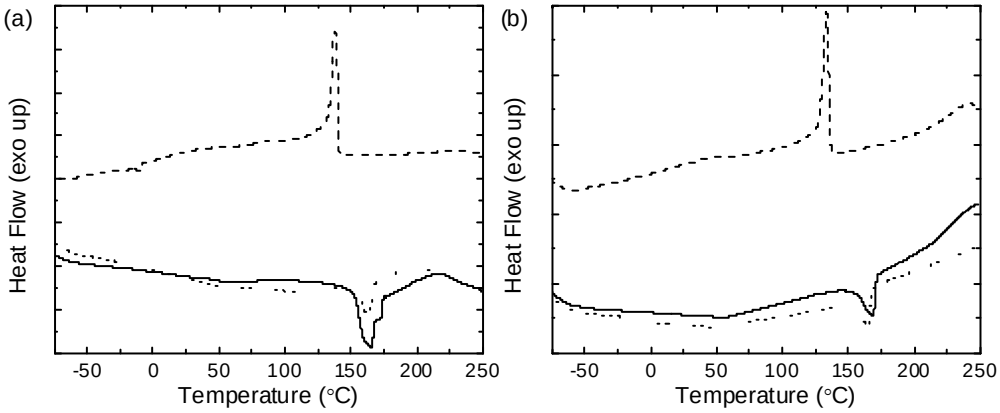

Figure 7. Differential scanning calorimetry (DSC) traces of neat macromonomer **1** (a) and **1·[Zn(NTf$_2$)$_2$]$_{1.0}$** (b). Traces from first heat (solid), first cool (dash), and second heat (dot). Experiments were conducted under N_2 at a heating rate of 10 °C/min.

Dynamic Mechanical Thermal Analysis. The mechanical properties of **1·[Fe(ClO$_4$)$_2$]$_{1.0}$**, **1·[Zn(ClO$_4$)$_2$]$_{1.0}$**, **1·[Zn(OTf)$_2$]$_{1.0}$**, and **1·[Zn(NTf$_2$)$_2$]$_{1.0}$** were investigated by dynamic mechanical thermal analysis (DMTA) (Figure 8). The thin films were heated at 3 °C/min and a frequency of 1 Hz under N_2. All films tested showed very similar mechanical properties with room temperature storage moduli of 440 MPa, 650 MPa, 420 MPa, and 470 MPa respectively. As with similar systems a continued decrease in the storage modulus is observed with increasing temperature, presumably stemming, in part, from the dynamic nature of the ligand:metal complex. The **1·[La(NTf$_2$)$_3$]$_{0.66}$** film proved to be more brittle than the films based on either Fe^{2+} or Zn^{2+}, and could not be characterized by DMTA temperature sweeps. The

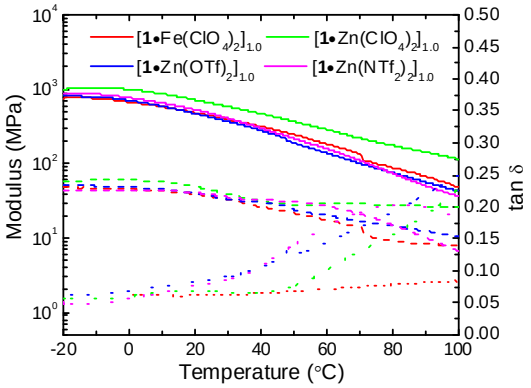

Figure 8. Dynamic mechanical thermal analysis (DMTA) temperature sweeps of **1·[Fe(ClO$_4$)$_2$]$_{1.0}$** (red), **1·[Zn(ClO$_4$)$_2$]$_{1.0}$** (green), **1·[Zn(OTf)$_2$]$_{1.0}$** (blue), and **1·[Zn(NTf$_2$)$_2$]$_{1.0}$** (magenta): storage modulus (solid line), loss modulus (dashed line), and tan d (dotted line). Experiments were conducted under N_2 at a heating rate of 3 °C/min and a frequency of 1 Hz.

brittle nature of the **1·[La(NTf$_2$)$_3$]$_{0.66}$** could stem the more dynamic of the Mebip:La^{3+} bond, which has resulted in weaker materials in previous studies.[12]

Synthesis and Characterization of Crosslinker 10. In order to test the effect of crosslinking while excluding the weaker binding lanthanide metals, an organic molecule (**8**) capable of crosslinking the metallo-supramolecular polymers was synthesized. Figure 9 shows the general synthetic route to access the tetrafunctional crosslinking molecule. The reactions involved the Sonogashira coupling of the alkyne Mebip ligand to aromatic halide cores, followed by diimide reduction. Initial attempts to carry out the reduction using literature procedures, namely toluene sulfonyl hydrazide (TSH) and tripropyl amine (TPA) in toluene, yielded only mixtures of partially reduced products. As discussed above, this reaction works well with electron-rich alkynes, such as the reduction of **2** in the synthesis of **1**. It was hypothesized that the relative electron deficient, and therefore less reactive, nature of the alkynes in the crosslinker **9** was the cause of the incomplete reactions here. The proposed mechanism for this reduction involves the TPA-catalyzed thermal decomposition of TSH to generate diimide (N_2H_2) in situ, which in turn hydrogenates the triple bond. The reduction step competes with the reaction of two diimide molecules to yield N_2 and hydrazine (N_2H_4). This reaction could become dominant if the decomposition of TSH is too fast and/or the alkyne is of low reactivity. Working with the hypothesis that this is the case for the systems at hand, a series of model reactions was set-up to establish conditions which would allow one to extend the Hahn reduction method to the reduction of electron-deficient alkynes. The results of our study clearly demonstrate that this is possible by a change to solvent that slows down the decomposition process of TSH[13] (*o*-dichlorobenzene) and the use of a less basic amine, which presumably results in a slower

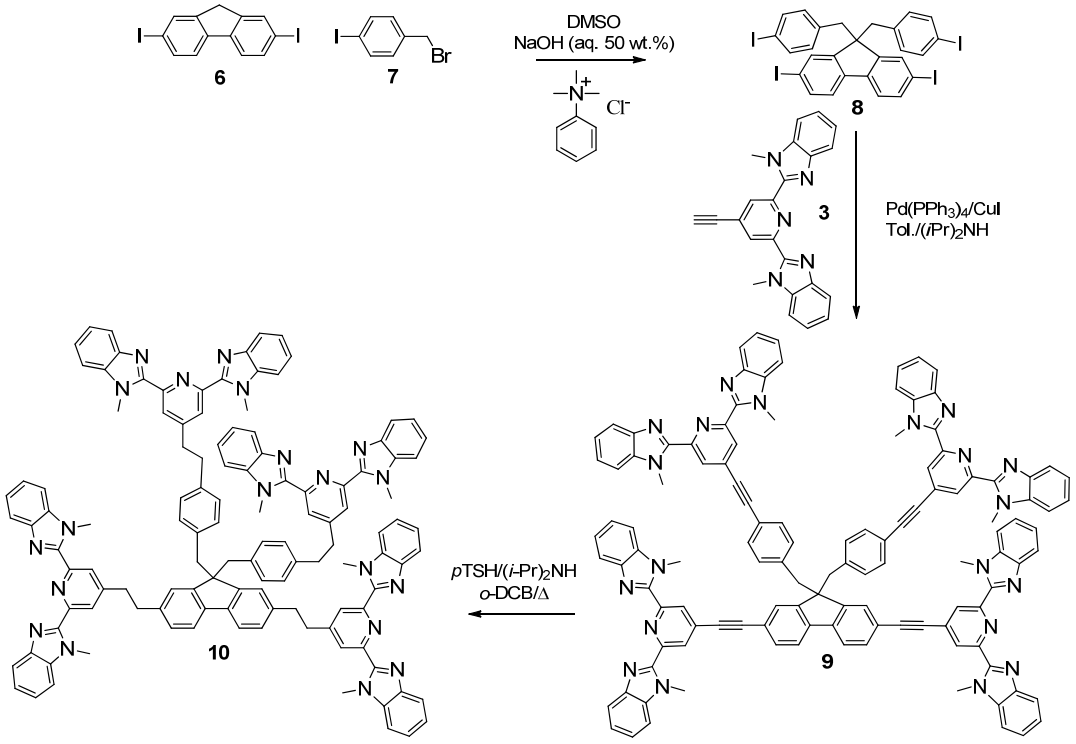

Figure 9. Synthesis of crosslinker **10**.

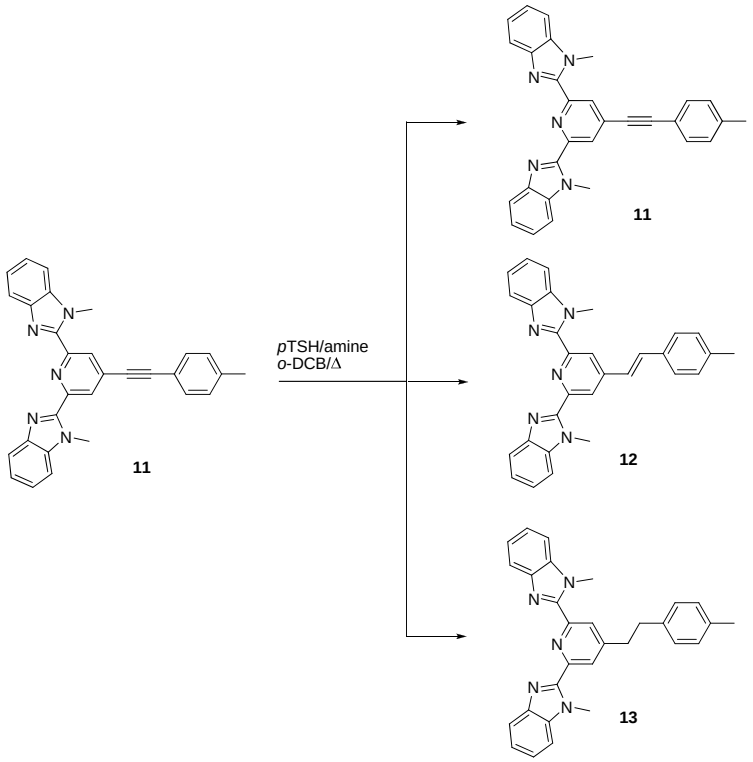

Amine	11 (%)	12 (%)	13 (%)
-	33	14	48
$(CH_3CH_2CH_2)_3N$	17	8	75
$(i\text{-Pr})_2NH$	3	1	96
$(n\text{-Bu})_2NH$	6	1	93

Figure 10. Effect of amine used on the yield of model compound **11**, with relative percents of **11**, **12**, and **13**, as measured by ^{1}H NMR integral ratios of the pyridine proton at 8.50, 8.48, and 8.31 ppm respectively.

decomposition rate of the TSH dramatically increases the effectiveness of the reduction. Figure 10 shows a selection of these reactions and illustrates the importance of the choice of amine. Using the new protocol, which appears to be a broadly applicable and an important extension of the original Hahn reduction method, it was possible to synthesize crosslinker **10**, which could not be accessed using the previous reaction conditions (Figure 9).

Dynamic Mechanical Thermal Analysis of Crosslinked Films. To test the effects that **10** has on the mechanical properties, a film composed of 90 mol% **1** and 10 mol% **10**, was prepared with $Zn(OTf)_2$ as the metal component ($[\mathbf{1}_{0.9}\mathbf{10}_{0.1}]\cdot[\mathbf{Zn(OTf)_2}]_{1.0}$). The mechanical properties of the thin film were tested by DMTA with a heating rate of 3 °C/min and a frequency of 1 Hz under N_2. Interestingly, it was found that at 10 wt% the crosslinker, **10**, had little effect on the mechanical properties (Figure 11). Unlike other ditopic systems, based on low Tg macromonomers,[14] the mechanical properties of this film appear to be based primarily on the crystalline nature of the polymeric core, with little effect from metal counter-ion, or crosslinking.

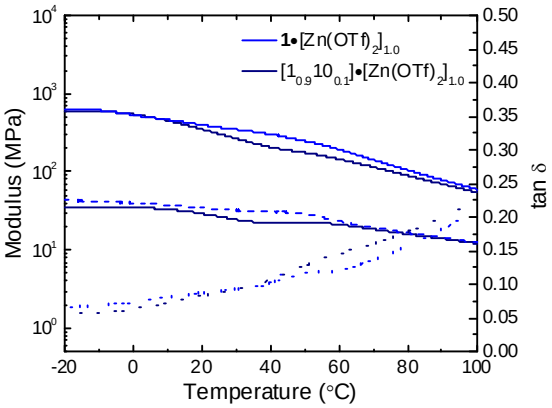

Figure 11. Dynamic mechanical thermal analysis (DMTA) temperature sweeps of $\mathbf{1}\cdot[\mathbf{Zn(OTf)_2}]_{1.0}$ (blue), and $[\mathbf{1}_{0.9}\mathbf{10}_{0.1}]\cdot[\mathbf{Zn(OTf)_2}]_{1.0}$ (dark blue): storage modulus (solid line), loss modulus (dashed line), and tan δ (dotted line). Experiments were conducted under N_2 at a heating rate of 3 °C/min and a frequency of 1 Hz.

Conclusions

Improved synthetic methods have allowed for the development of metallo-supramolecular films based on poly(*p*-xylylene) with varying metals and counterions. We have demonstrated that these metallosupramolecular polymers are relatively insensitive to type of metal ion salt used to assemble these materials suggesting that the properties are primarily based on the macromonomer. In this case the dominant factor on the mechanical properties appears to be the crystallization of the polymeric core or alkyl side chains. Improvement in the synthetic protocols for the Hahn reduction reaction allowed for the synthesis of an organic crosslinking molecule. Addition of this molecule did not produce any significant increase in the stiffness of the material, again highlighting that the mechanical properties of the material are governed by the nature of the polymeric backbone.

2.2. Photo-healable Metallo-supramolecular Polymers

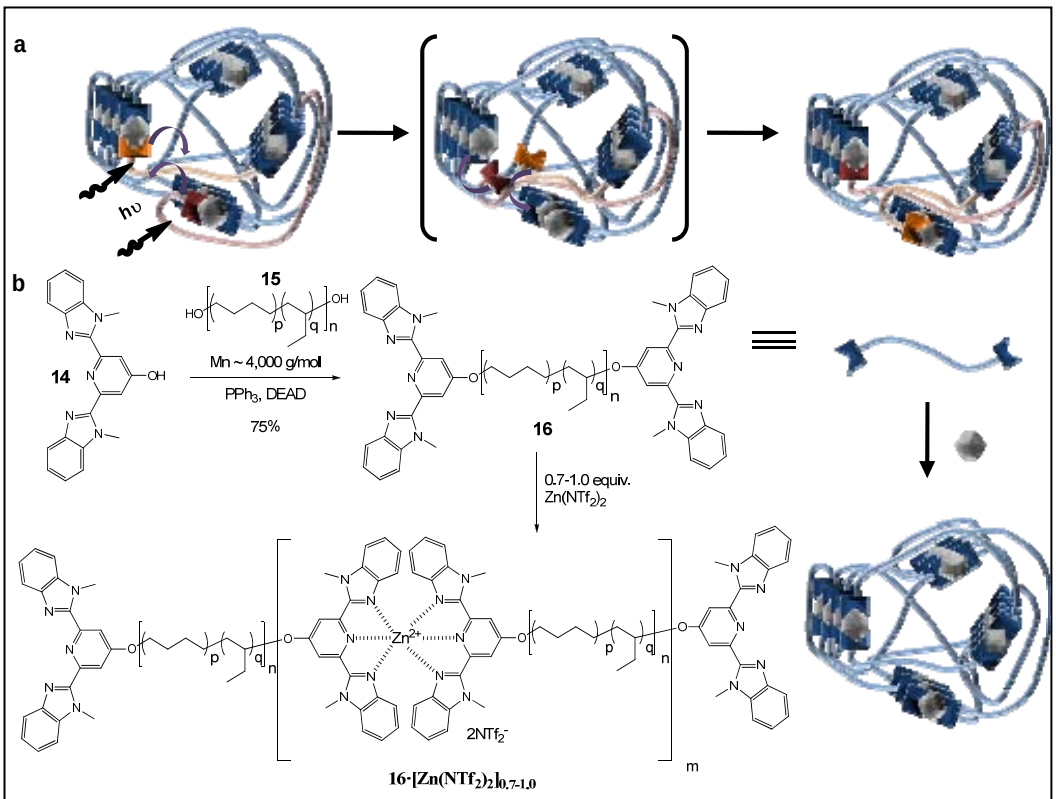

Figure 12. Photo-healable metallo-supramolecular polymers proposed mechanism and synthesis. a, Schematic representing optical healing of a metallo-supramolecular phase separated network. **b**, Synthesis of macromonomer **16** from **14** and **15,** and polymerization by addition of $Zn(NTf_2)_2$.

The healing of cracks in amorphous polymers by heating above the glass transition temperature (T_g) involves the steps of surface rearrangement and approach, wetting, diffusion, and re-entanglement of polymer chains.[15] The latter two steps are rate-limiting and paramount to restoring the material's original mechanical properties. The healing of polymers is therefore generally slow and inefficient, unless the molecular weight can be reduced during healing. This problem can be solved with polymers based on thermally reversible covalent[16,17] and non-covalent supramolecular motifs,[19] where the molecular weight can be temporarily reduced by shifting the reaction equilibrium to lower molecular weight species[20] by exposure to heat. This reduces the viscosity of the material, so that defects can be mended, before the equilibrium is shifted back and the polymer is reformed. Supramolecular materials that phase-separate into physically cross-linked networks (Figure 12a) should be especially well-suited for this purpose, since such structures are generally characterized by high toughness. At the same time, the supramolecular motifs can disengage in the solid-state upon exposure to heat or a competitive binding agent,[21,22] resulting in disassembly into small molecules[23] and dramatic viscosity reductions.. Reporting a series of new supramolecular materials formed by metal-ligand interactions, we demonstrate here that this architecture is an excellent basis for elastomeric materials in which defects can be quickly and efficiently repaired. We show that the use of light, which was recently exploited for healing of thermoset polymers using irreversible chemistry,[24] as a stimulus for the dissociation of supramolecular motifs has distinct advantages over thermally-healable systems, including the possibility of limiting the healing to only the damaged region.

The new polymers are based on a ditopic macromonomer (**16**) comprised of a poly(ethylene-*co*-butylene) core and two 2,6-bis(1'-methylbenzimidazolyl)pyridine (Mebip) ligands at the termini (Figure 12b). This macromonomer was synthesized via a Mitsunobu reaction of 2,6-bis(1'-methylbenzimidazoyl)-4-hydroxypyridine (**14**) and a hydroxyl terminated poly(ethylene-*co*-butylene) (**15**, number-average molecular weight, M_n, = 3500 g/mol). The hydrophobic, rubbery-amorphous nature of the latter was expected to cause phase-separation from the metal-ligand binding motif[25], and Mebip was chosen because several Mebip:metal complexes were already successfully self-assembled into polymeric materials,[26,27] and its optical properties appeared appropriate for photo-induced healing (vide infra). To probe the effect of the metal ion complex on the healing process, **16** was polymerized with $Zn(NTf_2)_2$ and $La(NTf_2)_3$. La^{3+} ions form weaker, more dynamic 3:1 complexes with the Mebip than Zn^{2+}, which binds with the ligand in a 2:1 ratio.[22,30] Bistriflimide (NTf_2^-) was chosen as the counter ion because of its thermal stability and non-coordinating nature. The combination of equimolar amounts of $Zn(NTf_2)_2$ and **16** in solution resulted in a rapid viscosity increase, indicative of supramolecular assembly (this polymer is denoted as **16·[Zn(NTf$_2$)$_2$]$_{1.0}$**). Solvent evaporation and compression-moulding resulted in colourless films with appreciable mechanical properties, unlike **16**, which is a waxy solid. Using the same procedure, polymers with Zn^{2+}:**16** ratios of 0.9-0.7 were also made (**16·[Zn(NTf$_2$)$_2$]$_{0.9}$**, **16·[Zn(NTf$_2$)$_2$]$_{0.8}$**, and **16·[Zn(NTf$_2$)$_2$]$_{0.7}$**).

Characterization of the supramolecular polymers based on **16** and $Zn(NTf_2)_2$ using small-angle X-ray scattering (SAXS) and transmission electron microscopy (TEM), carried out by Rick Beyer and Andrew J. Duncan at the U.S. Army Research Laboratory, Aberdeen Proving Ground, Maryland, revealed microphase-separated lamellar morphologies in

which the metal-ligand complexes form a "hard phase" that physically crosslinks "soft" domains formed by the poly(ethylene-*co*-butylene) cores. The SAXS data (Figure 13a) show multiple strong Bragg diffraction maxima at integer multiples of the scattering vector of the primary diffraction peak ($2q^*$, $3q^*$, etc.), characteristic of well-ordered layered morphologies. The lamellar period was found to be 8.3 nm for **16·[Zn(NTf$_2$)$_2$]$_{1.0}$** and to increase to 9.3 nm for **16·[Zn(NTf$_2$)$_2$]$_{0.7}$**. The number of strong reflections decreased from four to two as the Zn^{2+}:**16** ratio decreased from 1.0 to 0.7, indicating a significant degradation of long-range order. Microscopy confirmed lamellar morphologies for all compositions (Figure 13b) and the general reduction of long range order with decreasing metal content.

The thermal properties of the polymers based on **16** and Zn(NTf$_2$)$_2$ were probed by modulated differential scanning calorimetry. The MDSC trace of **16** shows reversible transitions at -51 and 47 °C, which by way of comparison with the MDSC traces of **2** and literature data[25] are assigned as T_g of the poly(ethylene-*co*-butylene) core and melting of phase-separated Mebip-domains. The MDSC trace of **16** further shows an irreversible transition at 193 °C, which is also observed in **15** and may be related to decomposition of a minor amount of residual double bonds in the poly(ethylene-*co*-butylene) core. The metallopolymers **16·[Zn(NTf$_2$)$_2$]$_x$** exhibit similar traces, but do not show melting of uncomplexed Mebip domains. Their thermo-mechanical properties were probed by dynamic mechanical thermal analysis. DMTA traces reveal the T_g of the poly(ethylene-*co*-butylene) core around -23 °C. A weaker transition around ~50 °C is also observed, which increases in magnitude with decreasing Zn^{2+} content, consistent with the dissociation of domains of uncomplexed Mebip, as observable in the MDSC of neat **16**. Below this transition, the polymers display storage moduli between 60-53 MPa with little dependence on the Zn^{2+}:**16** ratio. At higher temperatures the difference is more pronounced as polymers with lower metal content exhibit a larger drop of the storage modulus upon heating. The mechanical properties of the materials are significantly reduced at temperatures above 100 °C, indicative of depolymerization at higher temperatures. Stress-strain experiments conducted at 25 °C show a pronounced decrease in strength, elongation at break, and toughness as the Zn^{2+}:**3** ratio is decreased (Figure 14a,b). Overall, the mechanical data are consistent with the decrease of long range order with decreasing metal content (Figure 13a,b), and also reflect the molecular weight decrease resulting from offsetting the metal:ligand stoichiometry.

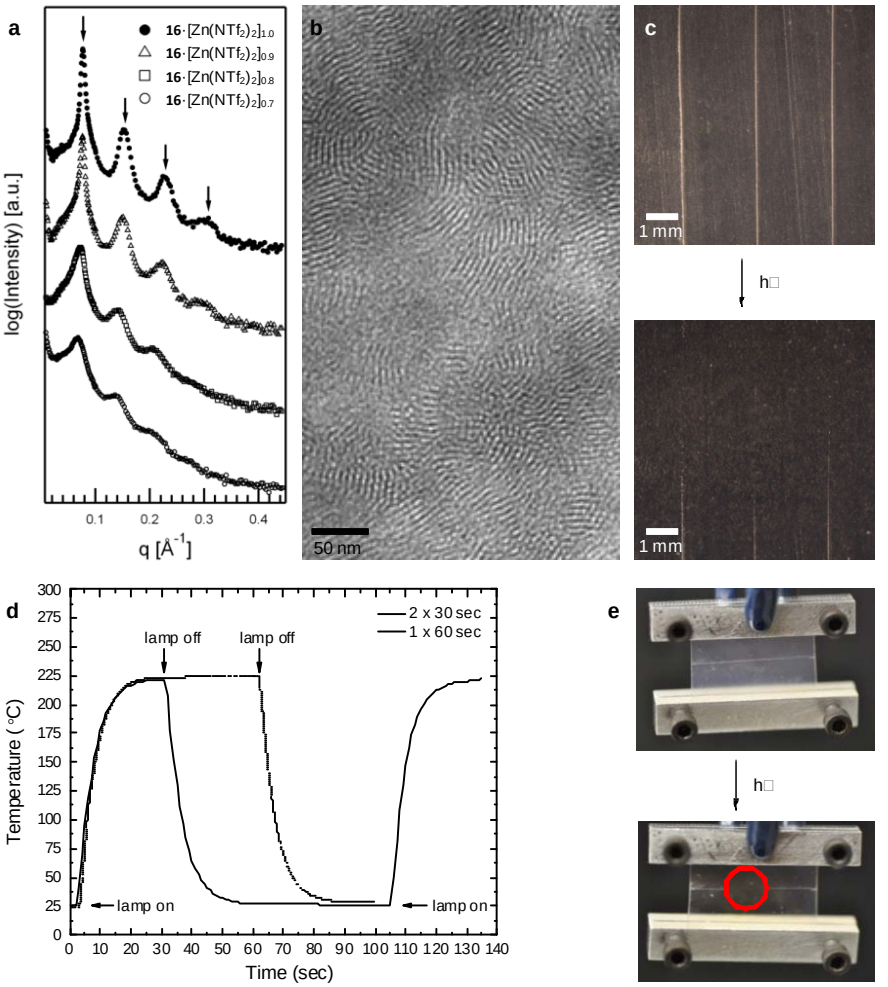

Figure 13. Characterization of Zn-based metallo-supramolecular polymers. a, SAXS data for metallo-supramolecular polymers of **16** with varying amounts of Zn(NTf$_2$)$_2$, shifted vertically for clarity. **b**, A representative TEM micrograph showing the lamellar morphology of **16·[Zn(NTf$_2$)$_2$]$_{1.0}$**. **c**, Optical healing of **16·[Zn(NTf$_2$)$_2$]$_{0.7}$** upon exposure to light in the wavelength range from 320-390 nm for 30 s twice at an intensity of 950 mW/cm^2. d, Optical healing of **16·[Zn(NTf$_2$)$_2$]$_{0.7}$** while under load ca. ~8 kPa.

In solution, the uncomplexed Mebip ligand in **16** displays a strong absorbance band with maximum at 313 nm. Upon complexation with $Zn(NTf_2)_2$, the intensity of this transition decreases and a new absorbance band at 341 nm appears. A titration series exhibits an isosbestic point around 328 nm, reflecting a well-defined equilibrium between free and metal-coordinated ligand. The absorption spectra of films of **16** and **16·[Zn(NTf$_2$)$_2$]$_x$** show similar features. Low-molecular weight Mebip:Zn^{2+} complexes fluoresce weakly, suggesting that a considerable portion of absorbed light is converted into heat. The optical healing pursued here is based on the assumption that this energy could be harnessed to dissociate the supramolecular motif locally and disengage the macromonomer ends from the hard phase (Figure 12a), which in turn should cause a decrease of the supramolecular polymer's molecular weight and locally liquefy the materials. To test this hypothesis, 350-400 μm thick films of the metallo-supramolecular polymers based on **16** and 0.7-1.0 equivalents of $Zn(NTf_2)_2$ were deliberately damaged by applying well-defined cuts with a depth of ca. 50-70% of the film thickness. These samples were subsequently exposed to UV irradiation with a wavelength of 320-390 nm and an intensity of 950 mW/cm^2. Pictures of the metallo-supramolecular polymer based on **16·[Zn(NTf$_2$)$_2$]$_{0.7}$** suggest that under these conditions two consecutive exposures of 30 s are sufficient to completely heal the cut without degrading the sample (Figure 13c), while materials with higher metal content appeared to heal less well (vide infra). Slight discoloration of the samples upon exposure to light was observed that increased with time; this may indicate some photooxidative stress, which is not surprising given the intensity, temperature, and presence of air and the possible presence of residual double bonds in the poly(ethylene-*co*-butylene) core. Figure 13e shows that it was readily possible to heal a **16·[Zn(NTf$_2$)$_2$]$_{0.7}$** film while applying a stress of ca. 8 kPa, by exposing only the damaged portion to the light. The extinction of the metallopolymers is ca. 890·cm^{-1} and light-absorption and heat generation therefore occurs at the surface of the films. The surface temperature upon UV exposure was probed with an IR-camera under conditions similar to those used for healing. Figure 2d shows, as an example, how the temperature of a **16·[Zn(NTf$_2$)$_2$]$_{0.7}$** film changed with time. Within 30 s the surface temperature increased to over 220 °C, a slight further increase was observed for extended irradiation times. In qualitative experiments it was confirmed that **16·[Zn(NTf$_2$)$_2$]$_{0.7}$** films could also be healed if upon heating to above ca. 190 °C, which supports that the proposed photo-thermal conversion is indeed the basis for healing. Reference experiments in which **16·[Zn(NTf$_2$)$_2$]$_{0.7}$** films were irradiated with light of similar intensity but a wavelength outside the absorption of the metal-ligand complex showed no healing, confirming that the process is indeed due to metal-ligand complex absorption and not infrared heating.

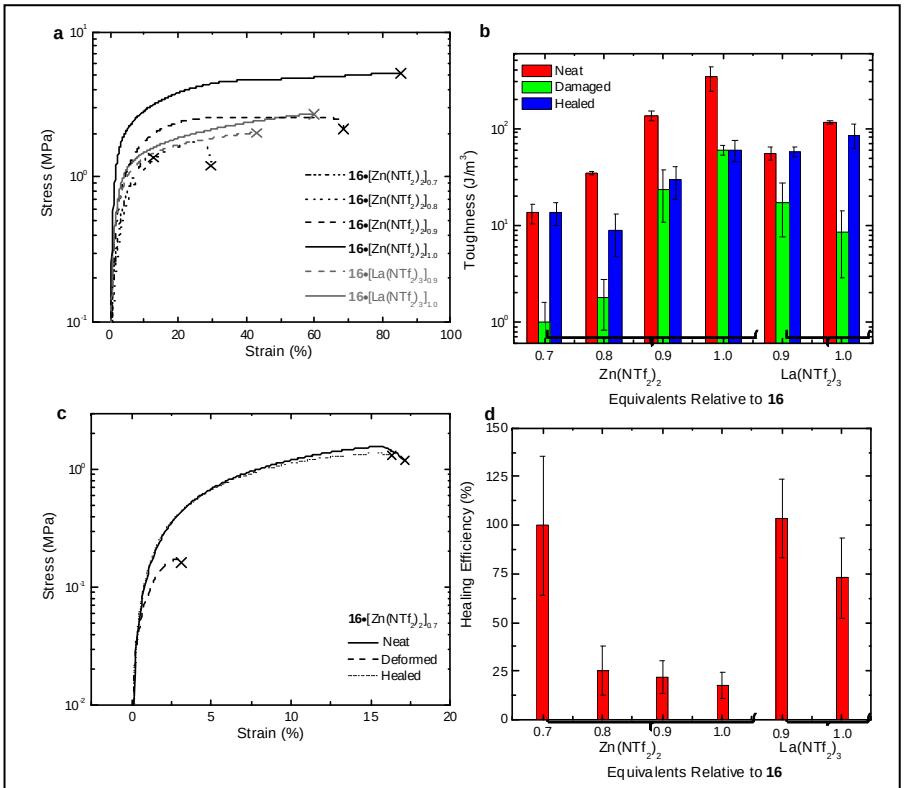

Figure 14. Mechanical and healing properties of the metallo-supramolecular polymers. a, Stress-strain curves of metallo-supramolecular polymers of **16** and varying amounts of $Zn(NTf_2)_2$ or $La(NTf_2)_3$. **b**, Toughness (T) of metallo-supramolecular polymers of **16** and varying amounts of $Zn(NTf_2)_2$ or $La(NTf_2)_3$. **c**, Stress-strain curves of films of **16·[Zn(NTf$_2$)$_2$]$_{0.7}$**; shown are data for original, damaged, and healed samples. **d**, Healing efficiency of films of **16** and varying amounts of $Zn(NTf_2)_2$ or $La(NTf_2)_3$.

To determine the healing efficiency of **16·[Zn(NTf$_2$)$_2$]$_x$** in a quantitative manner, films were damaged and healed as described above. Mechanical tests (stress-strain experiments) were conducted on original, damaged, and healed samples and the healing efficiency was expressed using toughness (T) as the figure of merit according to Equation 1:

$$\text{Healing Efficiency} = (T_{\text{healed}})/(T_{\text{original}}) \times 100 \qquad (1)$$

Figure14 shows that the strain and stress at break of a **16·[Zn(NTf$_2$)$_2$]$_{0.7}$** film (and hence T, which is determined by the area under the stress-strain curve) is significantly reduced upon damaging the sample by a cut as described above. Gratifyingly, the original properties could be restored upon light exposure. Statistical experiments (Figure 14b,d) show

that toughness of the healed sample set is comparable to that of the original sample set and statistically different from the toughness of the damaged sample set. The healing efficiency for this composition is 100 ± 36%. Lower healing efficiencies of 25 ± 12%, 22 ± 8.6%, and 18 ± 6.7% were observed for **16·[Zn(NTf$_2$)$_2$]$_{0.8}$**, **16·[Zn(NTf$_2$)$_2$]$_{0.9}$**, and **16·[Zn(NTf$_2$)$_2$]$_{1.0}$**. This is consistent with the greatest viscosity reduction in case of **16·[Zn(NTf$_2$)$_2$]$_{0.7}$**, on account of the excess of free ligands, which render the system more dynamic. The healing efficiency also correlates roughly with morphological long-range order. The materials having the best long range order, **16·[Zn(NTf$_2$)$_2$]$_{1.0}$** and **16·[Zn(NTf$_2$)$_2$]$_{0.9}$**, show poor healing efficiency, while the sample with the most disordered regions, **16·[Zn(NTf$_2$)$_2$]$_{0.7}$**, has the best healing behavior. The excellent optical healability of **16·[Zn(NTf$_2$)$_2$]$_{0.7}$** comes, however, at the expense of a slightly lower modulus and significantly lower stress and strain at break in comparison to **16·[Zn(NTf$_2$)$_2$]$_{1.0}$** (Figure 14a,b).

As La^{3+}:Mebip complexes are more labile and dissociate at lower temperatures than Zn^{2+}:Mebip complexes[21], metallo-supramolecular polymers based on **16** and either 1.0 or 0.9 equivalents of La(NTf$_2$)$_3$ (**16·[La(NTf$_2$)$_3$]$_{1.0}$** and **16·[La(NTf$_2$)$_3$]$_{0.9}$**) were also studied. Although titration experiments unequivocally showed that the La:MeBip(NTf$_2$)$_3$ complexes involve 1:3 metal:ligand binding, SAXS and TEM data reveal the formation of a predominantly lamellar-like morphology (Figure 15a,b) with a period of 7.4 nm (SAXS data for **16·[La(NTf$_2$)$_3$]$_{1.0}$**). The mechanical properties of these La^{3+}-containing supramolecular polymers are similar to those of **16·[Zn(NTf$_2$)$_2$]$_{0.9}$** (Figure 14), but their healing efficiencies of 104 ± 20% and 73 ± 21% for **16·[La(NTf$_2$)$_3$]$_{0.9}$** and **16·[La(NTf$_2$)$_3$]$_{1.0}$** (Figure 14b,d), are much better. The surface temperature of **16·[La(NTf$_2$)$_3$]$_{0.9}$** during healing of ca. 195 ˚C was lower than that of **16·[Zn(NTf$_2$)$_2$]$_{0.7}$** and optical microscopy showed qualitatively that the former liquefied more readily, consistent with the weaker and more dynamic binding. Thus, **16·[La(NTf$_2$)$_3$]$_{0.9}$** appears to exhibit the best combination of initial strength, strain to break and healing efficiency. It appears that this propensity is directly related to the more dynamic nature of the La:MeBip complexes vis a vis Zn:MeBip. A film of **16·[La(NTf$_2$)$_3$]$_{0.9}$** was repeatedly damaged and healed (Figure 15c,d) without any significant decrease of healing efficiency between cycles. Atomic force microscopy was used to probe the topology of a **16·[La(NTf$_2$)$_3$]$_{1.0}$** film around a defect before and after healing (Figure 15e-g). The images show that the cut is filled and disappears, consistent with the proposed viscosity decrease upon light exposure.

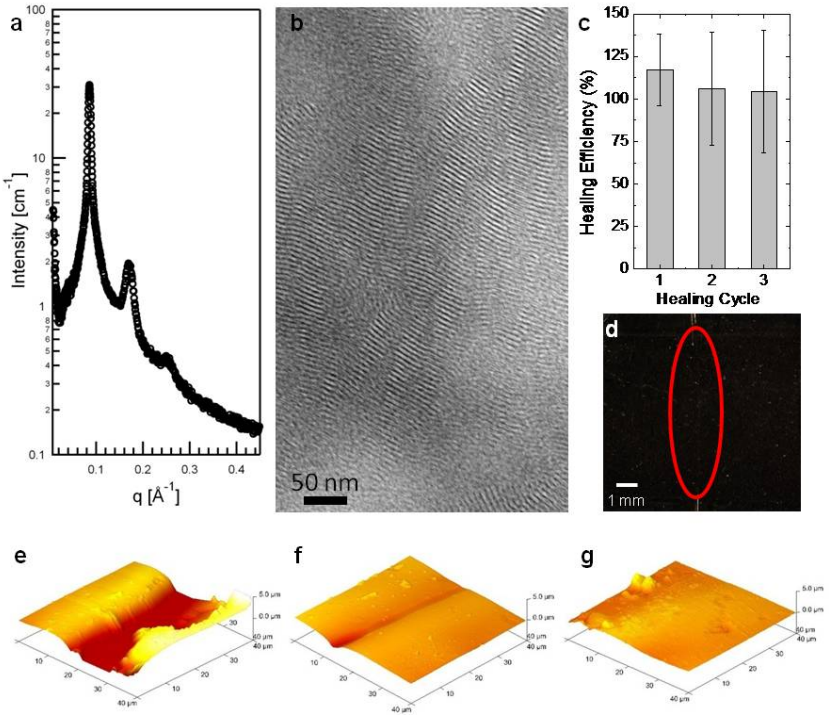

Figure 15. Characterization of La-based metallo-supramolecular polymers. **a**, SAXS data for metallo-supramolecular polymers of **16·[La(NTf$_2$)$_3$]$_{1.0}$**. **b**, A representative TEM micrograph shows the lamellar morphology observed in **16·[La(NTf$_2$)$_3$]$_{1.0}$**. **c**, Healing efficiency of multiple healing cycles for **16·[La(NTf$_2$)$_3$]$_{0.9}$**. **d**, Optical micrograph of **16·[La(NTf$_2$)$_3$]$_{0.9}$** after three healing cycles. **e-g**, AFM images of a damaged **16·[La(NTf$_2$)$_3$]$_{1.0}$** film before healing, after partially healing, and after complete healing, respectively.

Our systematic investigation of several strategically chosen compositions and in-depth morphological studies provide a first insight of the healing process in metallo-supramolecular polymers presented based on a previously unexplored combination of a supramolecular polymerization motif and the concept of light-heat conversion. The formation of lamellar morphologies in which a hard phase formed by the metal-ligand complexes physically cross-links the soft domains formed by the poly(ethylene-*co*-butylene) cores is the main determinant for the thermo-mechanical characteristics of the materials studied. The data suggest that the dynamics of the light-induced depolymerization, and thereby the healing behavior, are governed by the presence of an excess of free ligands and the nature of the metal-ligand bond. The concept of photo-thermal induced healing of supramolecular materials appears to be applicable to any supramolecular polymer with a binding motif that is sufficiently dynamic. The ability to change the chromophore allows tailoring the wavelength required for healing. The combination of the new approach with an additional mechanochromic response[31,32] promises access to true, that is autonomously functioning, self-healing materials, in which light is only absorbed at defect sites.

2.3. Decoupling Optical Properties in Metallosupramolecular Poly(*p*-phenylene ethynylene)s

In connection with experiments that target better phase segregation between the metal-ligand segment and the polymer building block (vide supra), we carried out the investigation of macromonomers in which the Mebip is separated from the rigid core through a flexible spacer. Thus a ditopic macromonomer **17** with a hexamethylene spacer in between the MeBip ligand and PPE (Figure 16) was prepared and metallosupramolecular polymers were produced through self-assembly with $Zn(ClO_4)_2$. The resulting materials display appreciable mechanical properties (in fact the modulus appears to be significantly increased compared to the reference material without spacer). We have previously shown that the addition of Zn^{2+} or Fe^{2+} ions to MeBip endcapped poly(phenylene ethynylene) (PPE) yields conjugated metallosupramolecular polymers with unparalleled mechanical properties. However, the optical and electronic properties of the conjugated core were significantly influenced upon metal binding. For example, the fluorescence of the PPE core was quenched and the resulting films showed little-to-no fluorescence as a result of energy transfer to the low-bandgap Mebip-metal moieties and nonradiative energy dissipation. Our new studies on metallopolymers based on **17** have shown that the optoelectronic functionalities of the semiconducting building blocks and metal ion 'chain-extenders' can be effectively de-coupled by the 'spacer-approach'.

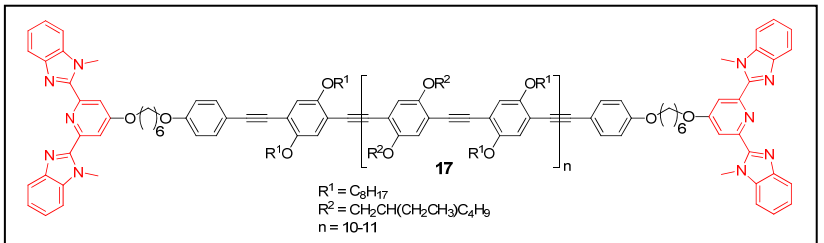

Figure 16. Chemical structure of the insulated macromonomer **17**.

Supramolecular Polymerization of Macromonomer 17 with Zn^{2+} and Fe^{2+}. The formation of metallo-supramolecular polymers of the type $[\mathbf{17}\cdot MX_2]_n$ is readily achieved by the addition of metal salts dissolved in CH_3CN to a $CHCl_3$ solution of macromonomer **17**. We employed Zn^{2+} and Fe^{2+}, with the intent to probe the influence of the different electronic characteristics of these metals on the resulting metallopolymers and to compare them with previously investigated materials.[27,33] Zn^{2+} features a fully occupied d-orbital ($3d^{10}$) and is a prototype for metals that show hardly any tendency for metal-to-ligand charge transfer (MLCT) with imine-type ligands.[34] In a number of different systems, we previously observed that the optical properties of phenylene ethynylene chromophores with imine-ligands display significant changes upon complexation to Zn^{2+}, most notably a significant reduction of the PL intensity and the development of orange luminescence.[27,33] We speculated that these changes might be suppressed by the introduction of a spacer between the chromophore and the ligand. By contrast, Fe^{2+} is well known to form pronounced MLCT complexes and to act as a strong fluorescence quencher.[35] We assumed that electronic interactions with the PPE backbone could be substantially reduced through the spacer, but anticipated PL quenching through Förster-type energy transfer between the PPE and the MLCT complex (vide infra).

Optical Properties of $[\mathbf{17}\cdot Zn(ClO_4)_2]_n$ and $[\mathbf{17}\cdot Fe(ClO_4)_2]_n$. With the goals of attaining further insights into the mechanism of the metal-mediated self-assembly processes of **17**, and to elucidate the effect of the spacer between Mebip ligand and PPE chromophore, $Zn(ClO_4)_2$ (Figure 17) and $Fe(ClO_4)_2$ (Figure 18) were titrated into solutions of **17** and the resulting products were analyzed by means of UV-Vis absorption and PL spectroscopy. Figure 9a reveals that the absorption arising from the PPE backbone is hardly changed upon addition of Zn^{2+}. However, a small increase of the absorption in the regime of 330 – 360 nm can be observed, which is interpreted with the formation of Zn-Mebip complexes.[27a] The inset of Figure 17a, which displays the absorption at 345.5 nm as a function of $[Zn^{2+}]$ shows that this transition intensifies linearly with the Zn^{2+} concentration. The molecular weight of the sample was calculated by correlating the point where the absorption at 345.5 levels off with a Zn^{2+}:**17** ratio of 1:1. This behavior is evidence for the formation of a metallo-supramolecular complex of the form $[\mathbf{17}\cdot Zn(ClO_4)_2]_n$, as it is required for the formation of the supramolecular polymer. Figure 17b demonstrates that, by contrast, the PL emission characteristics of **17** remain virtually unchanged upon addition of Zn^{2+}; the spectral features remain identical while the emission intensity experiences only a minor reduction.

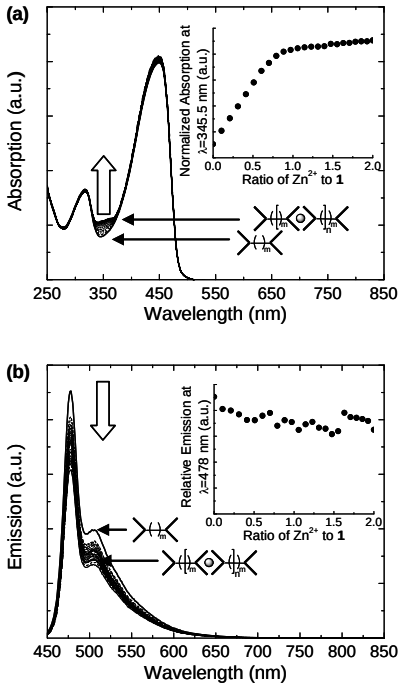

Figure 17. (a) UV-vis specta acquired upon titration of **17** (3 μM) in $CH_3CN/CHCl_3$ (1/9 v/v) with $Zn(ClO_4)_2$. The inset shows the absorption at 345.5 nm as a function of Zn^{2+}:**17** ratio. (b) PL emision specta acquired under excitation at 40 nm upon titration of **17** (3 μM) in $CH_3CN/CHCl_3$, (1/9 v/v) with $Zn(ClO_4)_2$. The inset shows the emission absorption at 345.5 nm as a function of Zn^{2+}:**17** ratio.

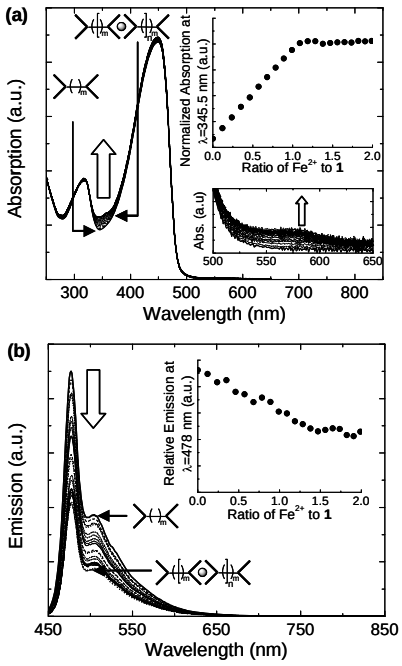

Figure 18. (a) UV-vis specta acquired upon titration of **17** (3 μM) in $CH_3CN/CHCl_3$ (1/9 v/v) with $Fe(ClO_4)_2$. The top inset shows the absorption at 345.5 nm as a function of Fe^{2+}:**17** ratio, the bottom inset is a 70x magnification showing the metal centered *d-d* transitions. (b) PL emision specta acquired under excitation at 40 nm upon titration of **17** (3 μM) in $CH_3CN/CHCl_3$ (1/9 v/v) with $Fe(ClO_4)_2$. The inset shows the emission absorption at 345.5 nm as a function of Fe^{2+}:**17** ratio.

This behavior is in marked contrast to that of a previously investigated metallopolymer of an otherwise identical structure, but without the hexamethylene spacers between the PPE core and the Mebip ligands. In that polymer, the luminescence was almost completely quenched and exhibited a significant bathochromic shift, as a result of strong electronic coupling between the PPE-based core and the Mebip-Zn^{2+} termini and efficient energy migration to the latter sites.[36] Thus, the hexamethylene spacers between the conjugated backbone and the Mebip groups indeed provide efficient "optical insulation" and de-couple the optical properties of the PPE backbone from the Mebip-Zn^{2+} complexes, which now merely function as 'chain extenders'.

The addition of Fe^{2+} to macromonomer **17** causes, at first glance, similar optical changes as observed for the addition of Zn^{2+}. As in the case of Zn^{2+}, the absorption spectrum (Figure 18a) shows a band between 330 and 375 nm that intensifies linearly with the Fe^{2+} concentration and levels off at a Fe^{2+}:**17** ratio of 1:1. At the same time, a weak but characteristic metal-to-ligand charge-transfer absorption band centered at ca. 575 nm can be observed, which is concomitant with the formation of a 2:1 Mebip-Fe^{2+} complex,[37] and indicative of a supramolecular polymer of the structure $[\mathbf{17}\cdot Fe(ClO_4)_2]_n$. Also in this case the features of the PL spectrum (Figure 18b) remain completely unchanged and the polymer remains highly luminescent upon introduction of Fe^{2+} – unlike virtually all other previously investigated supramolecular materials comprising Fe^{2+}. However, the emission intensity does decrease linearly with increasing Fe^{2+} concentration to level off at ca. 52 % of its original value at a ligand:metal ratio of ca. 2:1. This behavior suggests weak Förster-type energy transfer between the PPE core and the Mebip-Fe^{2+} endgroups, which provide pathways for non-radiative exciton decay. It appears possible to further minimize the effect by extending the spacer length and minimizing the overlap integral by appropriate molecular engineering.

The optical properties of spin-coated films of **17** and $[\mathbf{17}\cdot Zn(ClO_4)_2]_n$ are virtually identical (Figure 19), indicating that also in the solid state the optical insulation between the PPE backbone and the Mebip-Zn^{2+} complexes is maintained. The spectra show rather narrow, well-resolved emission bands that are characteristic for disordered samples which lack significant long-range order and specific intermolecular interactions. The PL spectrum broadens somewhat and experiences a significant bathochromic shift if films of $[\mathbf{17}\cdot Zn(ClO_4)_2]_n$ (Figure 19a) are produced by solution-casting. This is consistent with an increased degree of long-range order and mirrors the findings of studies in which samples of neat PPE of supramolecular metallo-PPEs were either processed under slow solvent evaporation or annealed.

In order to explore if the presence of the Mebip-Zn^{2+} complexes impacts the charge transport, we prepared single-layer light-emitting diodes (LEDs) based on $[\mathbf{17}\cdot Fe(ClO_4)_2]_n$, ITO, and Al, and compared the response of the devices with that of a single-layer device based on a polymer corresponding to the core employed here, i.e., a PPE featuring *n*-octyloxy and 2-ethylhexyloxy side chains in an alternating pattern (EHO-OPPE).[38] The *I-V* curves of LEDs based on $[\mathbf{17}\cdot Zn(ClO_4)_2]_n$ show typical rectifying behavior (Figure 19b) with an onset voltage of ca. 1.25 MV/cm) and a maximum brightness of ca. 29 cd/m^2 (similar to a comparable EHO-OPPE device). The

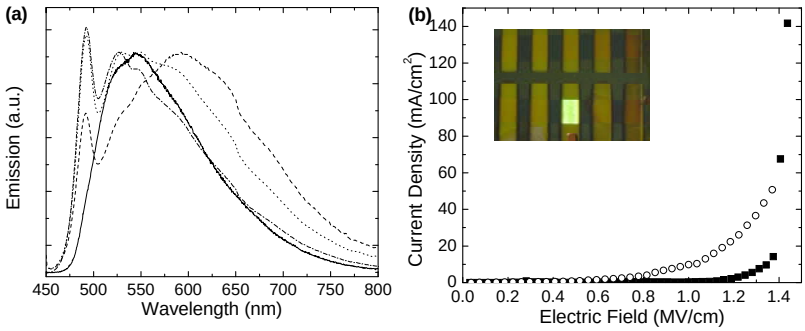

Figure 19. (a) PL emission spectra of solid state samples measured as a solution cast Zn^{2+}:**17** metallo-supramolecular polymer (dashed), spun-cast Zn^{2+}:**17** metallo-supramolecular polymer (dash-dot), spun-cast neat macromonomer **17** (dotted), and as a spun-cast metallo-supramolecular polymer Zn^{2+}:**17** LED (solid). (b) *I-V* curves of LEDs based on $[\mathbf{17}\cdot Zn(ClO_4)_2]_n$.

devices were found to emit yellow-green light (Figure 19b) with an emission maximum at 542 nm. The emission spectra that nicely match the PL spectra, indicating that indeed the same excited states are responsible for the respective emission processes. These devices are, of course, by no means optimized but the comparative experiment nicely demonstrates that the Mebip-Zn^{2+} complexes hardly, if at all, influence the charge transport in these LEDs.

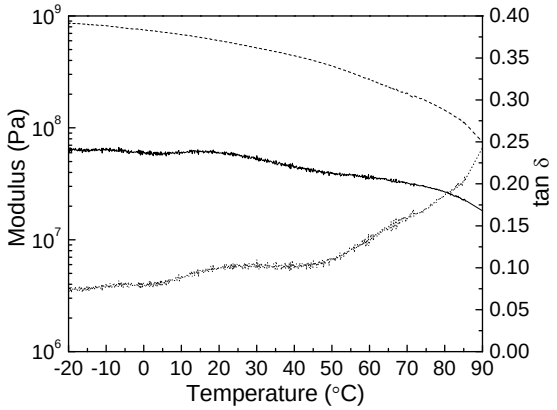

Figure 20. Dynamic mechanical thermoanalysis (DMTA) traces of Zn^{2+}:**17** metallo-supramolecular polymer. Loss modulus (dash) storage modulus (solid) and tan d (dot). Experiments were conducted under N_2 at a heating rate of 3 °C/min and a frequency of 1 Hz.

Mechanical Properties of $[\mathbf{17}\cdot Zn(ClO_4)_2]_n$. $[\mathbf{17}\cdot Zn(ClO_4)_2]_n$ displayed very good film-forming characteristics and objects produced from this polymer displayed appreciable mechanical properties (Figure 20) – quite in contrast to the parent macromonomer, which is rather brittle and does not have the ability to form self-supporting films. Thus, the mechanical properties of $[\mathbf{17}\cdot Zn(ClO_4)_2]_n$ were investigated in detail by means of dynamic mechanical thermoanalysis (DMTA, Figure 20). Experiments were conducted in a temperature range of -20 to 90 ºC, i.e. in a regime in which both the PPE core[39] and the Mebip-Zn^{2+} complexes are thermally stable. The loss and storage moduli of $[1\cdot Zn(ClO_4)_2]_n$ were determined to be ca. 860 and ca. 62 MPa at -20 ºC and ca. 560 and ca. 57 MPa at 25 ºC respectively. A decrease of the moduli was observed over the experimental temperature range. The tanδ curve suggest a transition above approximately 50 ºC, which in view of the striking similarity to the traces of a high-molecular poly(*p*-2,5-dialkoxy phenylene ethynylene) (M_n ~ 83,000 g mol^{-1})[39] reported before, we tentatively assign to a glass transition. Interestingly, the room-temperature moduli are much higher than those of a previously investigated metallopolymer of an otherwise identical structure, but without the hexamethylene spacers between the PPE core and the Mebip ligands.

References

1 For recent reviews see: (a) Lohmeijer, B.G.G.; Schubert, U.S. *J. Polym. Sci., Part A: Polym. Chem.* **2003**, *41*, 1413. (b) Dobrawa, R.; Würthner, F. *J. Polym. Sci., Part A: Polym. Chem.* **2005**, *43*, 4981-4995. (c) Holliday, B.J.; Swager, T.M. *Chem. Comm.* **2005**, 23. (d) Friese, V.A.; Kurth, D.G. *Coord. Chem. Rev.* **2008**, *252*, 199. (e) Fox, J.D.; Rowan, S.J. *Macromolecules* **2009**, *42*, 6823-6835.

2 Knapton, D.; Iyer, P.K.; Rowan, S.J.; Weder, C. *Macromolecules* **2006**, *39*, 4069-4075.

3 (a) Beach, W.F. Xylylene Polymers. In *Encyclopedia of Polymer Science and Technology*, 3rd ed.; Kroschwitz, J., Ed.; John Wiley & Sons: New York, 2004; Vol. 12, p 587 ff. (b) Greiner, A.; Mang, S.; Schäfer, O.; Simon, P. *Acta Polym.* **1997**, *48*, 1-15.

4 Errede, L. A.; Szwarc, M. *Q. Rev. Chem. Soc.* **1958**, *12*, 301.

5 Beach, W. F. in *Encyclopedia of Polymer Science and Technology*, 3rd ed.; J. Kroschwitz, ,Ed.; John Wiley & Sons: New York, **2004**; *Vol. 12*, p. 587 ff.

6 Greiner, A.; Mang, S.; Schäfer, O.; Simon, P. *Acta Polym.* **1997**, *48*, 1.

7 (a) Errede, L. A.; Knoll, N. *J. Polym. Sci.* **1962**, *60*, 21 (1962). (b) Kirkpatrick, D. E.; Wunderlich, B. *Makromol. Chem.* **1985**, *186*, 2595.

8 Szwarc, M. *Polym. Eng. Sci.* **1976**, *16*, 473.

9 Greiner, A. *Trends Polym. Sci.* **1997**, *5*, 12.

10 McKenzie, B.M.; Miller, A.K.; Wojecki, R.J.; Johnson, J.C.; Burke, K.A; Tzeng, K.A.; Mather, P.T.; Rowan, S.J. *Tetrahedron* **2008**, *64*, 8488-8495.

11 Bunz, U.H.F. et al. *Chem. Mater.* **1999**, *11*, 1416.

12 Knapton, D.; Burnworth, M.; Rowan, S.J.; Weder, C. *Angew. Chem. Int. Ed.* **2006**, *45*, 5825-5829.

13 Nakagawa, T; Makotot, O. J. *J. Polym. Sci., Part A: Polym. Chem.***1968**, *6*, 1795.

14 (a) Beck, J. B.; Rowan, S. J. *J. Am. Chem. Soc.* **2003**, *125*, 13922. (b) Zhao, Q. Y.; Beck, J. B.; Rowan, S. J.; Jamieson, A. M. *Macromolecules* **2004**, *37*, 3529. (c) Rowan, S. J.; Beck, J. B. *Faraday Discuss.* **2005**, *128*, 43. (d) Beck, J. B.; Ineman, J. M.; Rowan, S. J. *Macromolecules* **2005**, *38*, 5060. (e) Weng, W.; Beck, J. B.; Jamieson, A. M.; Rowan, S. J. *J. Am. Chem. Soc.* **2006**, *128*, 1163.

15. Kim, Y. H.; Wool, R. P. *Macromolecules* **1983**, *16*, 1115-1120.

16. Chen, X., *et al. Science* **2002**, 295, 1698-1702.

17. Murphy, E. B., *et al. Macromolecules* **2008**, *41*, 5203-5209.
18. Burattini, S., *et al. Chem. Commun.* **2009**, 6717-6719.
19. Burattini, S., *et al. J. Am. Chem. Soc.* **2010**, *132*, 12051-12058.
20. Wojtecki, R.J.; Meador, M.A.; Rowan S.J. *Nature Materials* **2011**, 10, 14-27.
21. Bosman, A. W., Sijbesma, R. P.; Meijer, E. W. *Mater. Today* **2004**, *7*, 34-39.
22. Kumpfer, J. R., Jin, J. Z.; Rowan, S. J. *J. Mater. Chem.* **2010**, *20*, 145-151.
23. Sivakova, S., Bohnsack, D. A., Mackay, M. E., Suwanmala, P.; Rowan, S. J. *J. Am. Chem. Soc.* **2005**, *127*, 18202-18211.
24. Ghosh, B.; Urban, M. W. *Science* **2009**, *323*, 1458-1460.
25 . Kautz, H., van Beek, D.J.M., Sijbesma, R.P.; Meijer, E.W. *Macromolecules* **2009**, *39*, 4265-4667.
26. Beck, J. B., Ineman, J. M.; Rowan, S. J. *Macromolecules* **2005**, *38*, 5060-5068.
27 (a) Iyer, P.K.; Beck, J.B.; Weder, C.; Rowan, S.J. *Chem. Comm.* **2005**, 319-321. (b) Knapton, D.; Rowan, S.J.; Weder, C. *Macromolecules* **2006**, *39*, 651-657. (c) Burnworth, M.; Knapton, D.; Rowan, S.J.; Weder, C. *J. Inorg. Organomet. Polym. Mat.* **2007**, *17*, *40*, 91-103.
28. Burnworth, M., Mendez, J. D., Schroeter, M., Rowan, S. J.; Weder, C. *Macromolecules* **2008**, *41*, 2157-2163.
29. Knapton, D., Rowan, S. J.; Weder, C. *Macromolecules* **2006**, *39*, 651-657.
30. Beck, J. B. & Rowan, S. J. *Faraday Dis.* **2005**, *128*, 43-53.
31. Kunzelman, J., Kinami, M., Crenshaw, B. R., Protasiewicz, J. D.; Weder, C. *Adv. Mater.* **2008**, *20*, 119-122.
32. Crenshaw, B. R., *et al. Macromolecules* **2007**, *40*, 2400-2408.
33 Kokil, A.; Yao, P.; Weder, C. *Macromolecules* **2005**, *38*, 3800-3807.
34 Jaeger, F.M.; van Dijk, J.A. *Z. Anorg. Ch.* **1938**, *227*, 273.
35 Dobrawa, R.; Wuerthner, F. *Chem. Comm.* **2002**, 1878-1879.
36 (a) Zhou, Q.; Swager, T.M. *J. Am. Chem. Soc.* **1995**, *117*, 12593-12602. (b) Swager, T.M. *Acc. Chem. Res.* **1998**, *31*, 201-207.
37 (a) Krumholz, P. *Inorg. Chem.* **1965**, *4*, 612-616. (b) El-ghayoury, A.; Schenning, A.P.H.J.; Meijer, E.W. *J. Polym. Sci.: Part A: Polym. Chem.* **2002**, *40*, 4020-4023.
38 Montali, A.; Smith, P.; Weder, C. *Synth. Met.* **1998**, *97*, 123.
39 Steiger, D.; Smith, P.; Weder, C. *Macromol. Rapid Commun.* **1997**, *18*, 643-649.